World Academy of Science, Engineering and Technology
International Journal of Materials and Metallurgical Engineering
Vol:11, No:3, 2017

Nanocharacterization of PIII Treated 7075 Aluminum Alloy

Bruno Bacci Fernandes, Stephan Mändl, Ataíde Ribeiro da Silva Junior, José Osvaldo Rossi, Mário Ueda

Open Science Index, Materials and Metallurgical Engineering Vol:11, No:3, 2017 publications.waset.org/10006624.pdf

Abstract**—**Nitrogen implantation in aluminum and its alloys is acquainted for the difficulties in obtaining modified layers deeper than 200 nm. The present work addresses a new method to overcome such a problem; although, the coating with nitrogen and oxygen obtained by plasma immersion ion implantation (PIII) into a 7075 aluminum alloy surface was too shallow. This alloy is commonly used for structural parts in aerospace applications. Such a layer was characterized by secondary ion mass spectroscopy, electron microscopy, and nanoindentation experiments reciprocating wear tests. From the results, one can assume that the wear of this aluminum alloy starts presenting severe abrasive wear followed by an additional adhesive mechanism. PIII produced a slight difference, as shown in all characterizations carried out in this work. The results shown here can be used as the scientific basis for further nitrogen PIII experiments in aluminum alloys which have the goal to produce thicker modified layers or to improve their surface properties.

Keywords**—**Aluminum alloys, plasma immersion ion implantation, tribological properties, hardness, nanofatigue.

I. Introduction

TRANSPORTATION systems have required new lightweight materials to increase speed and efficiency, as well as to support higher temperatures and friction [1]. Aluminum is almost the lighter metal and nowadays many advanced alloys are produced using it. Other problems that must be overcome by light materials are those concerning corrosion in different environments. Improvements in these applications may be obtained by studies on composition, processing, microstructure and properties of such materials [1].

Surface contact fatigue is crucial to study bearings or railway tracks, mainly because of spalling [2]. Other applications do not allow even small amounts of wear, such as in hard disc drives and microelectromechanical devices [3]. Another important research field is the development of nanostructured materials, and AlN has attracted interest in optoelectronics, high-temperature electronics and acousto-electronics [4]. Nanoindentation was developed to make possible mechanical measurements of thin films even on complex surfaces. This new technique examines loads and displacements of a very small tip that is pressed at the surface. Semiconductor and magnetic storage industries employ it in materials having roughness values of tens of nanometers [5]. By correlating experimental and computational results, nanoindentation can be considered a non-destructive and rapid procedure from which the stress-strain response of a given thin film is ascertained [6].

Standing contact fatigue has been employed to verify the mechanism for surface fatigue based on the cyclic tensile surface stresses [2]. Currently, such a topic has been attracting much interest to produce fatigue crack nucleation and growth [7]. Modelling works shows that pressure profiles are significantly different from equivalent Hertz profiles using indentations with loads up to 300 times the load necessary for initial yield. Subsequent load cycles produce continued yielding almost entirely within the plastically deformed region that was made by the first load. The increase in plastic strain decreases with each subsequent half-cycle [3]. Some important information based on nanoindentation of hard material must be highlighted, as for example that the formation of ring crack is favored by a positive radial stress, which in turn is reduced by the unloading. The hoop stress is rather increased and becomes more tensile by unloading, which is a reason to the formation of radial cracks. Radial stresses become more compressive on unloading; however, they are initially higher than the hoop stresses, producing conditions for nucleation and initial growth of ring cracks. When the radius of the elastic-plastic boundary is equal to or greater than the radius of the contact circle, the sign of the radial and hoop stresses is reversed [7]. If a brittle specimen has not fractured during indentation to maximum load it frequently fails during unloading [2], [7]. In such a contest, PIII is interesting because of its non-directional characteristic, as well as for making possible batch processes [8]-[10]. PIII has been used for treating several materials such as alloys based on iron, titanium and aluminum. There are several problems on the surface treatments of aluminum, such as the dense Al_2O_3 film of 10 nm that forms naturally due the contact with air [11], [12]. Also, some aluminum alloys are highly temperature-sensitive because of a tempering step in their fabrication, for example, the 7075 T6 alloy (Al-Cu-Mg-Zn) that is tempered at 120 ^oC [13].

Nitrogen PIII at 15 keV (150 minutes, 400 Hz and 20 μs) can produce AlNO phases on the sub-surface of 5052 alloy [14]. However, hardness reduction is verified due to the relatively high temperature reached in the PIII process (around 400 ^oC). Hybrid treatments or high voltage PIII already

The authors are with the Instituto Nacional de Pesquisas Espaciais, LAP/INPE, Av. dos Astronautas 1758, Caixa Postal 515, São José dos Campos, SP, Brazil.

Stephan Mändl is with the Leibniz-Institut für Oberflächenmodifizierung e.V., Permoserstraße 15, 04318, Leipzig, Germany.

Bruno Bacci Fernandes is with the Leibniz-Institut für Oberflächenmodifizierung e.V., Permoserstraße 15, 04318, Leipzig, Germany and with the Bruno Bacci Fernandes is with the Universidade Braz Cubas, Av. Francisco Rodrigues Filho, 1233, CEP 08773-380, Mogi das Cruzes, SP, Brazil (Contact Author, phone: +55 12 3208 6698; e-mail: baccicss@gmail.com).

Open Science Index, Materials and Metallurgical Engineering Vol:11, No:3, 2017 publications.waset.org/10006624.pdf

demonstrated significant surface improvements on aluminum materials without softening effects [15]-[17]. Studies show that PIII experiments with temperatures below 200 ºC, short pulses (1.5 μs) and high voltage application (above 35 kV) keep the pristine hardness and improve corrosion/wear properties of aluminum alloys [18]-[21].

This work reports details of the nitrogen PIII treatment in 7075 AA (aluminum alloy) using a novel device to protect the surface from residual water. Nanoindentation experiments are also presented here and related to physical and chemical characterizations.

II. Experimental Procedures

The 7075 AA sample disks of 15-mm diameter and 3-mm thickness were polished (Ra= 50 nm) and cleaned in ultrasound acetone bath. The experimental set-up for the nitrogen PIII is shown elsewhere [22]-[24] with HV pulses of 40 kV, 100 Hz and 1 μs that produces a temperature below 200 ºC. Argon plasma was performed to clean the residual oxygen that keep inside the evacuated chamber. As protection against contamination of the surface samples at this cleaning stage, a shield was employed. After that, this shield was removed from the front of the surface samples before the beginning of the nitrogen implantation without breaking the vacuum. Work pressure of 10^{-3} torr (1 Pa) for 60 min was applied to the samples.

XRD measurements were obtained by a Philips diffractometer (model X'Pert) in the standard 2θ mode (voltage of 40 kV and current of 45 mA). The surface structures of the samples were characterized using a SEM, where compositional analysis was carried out by the energy dispersive spectroscopy (EDS). Surface morphology and roughness were analyzed by AFM and optical profilometry.

Tribological evaluations of the sample surfaces were conducted with a TriboScope nanomechanical indentation tester from Hysitron Inc. Measurements of dry friction coefficient were accomplished by an oscillating ball-on-disk tribometer. Parameters used for this test were: load of 0.5 N with a 4.7-mm diameter alumina ball as a counterpart material, average speed of 1 cm/s and track length of 4 mm. The worn-out surfaces were examined under the SEM in the secondary electron mode to find out the wear mechanisms in PIII treated and untreated samples.

The nitrogen depth profiles were measured using time-of-flight secondary ion mass spectrometry (ToF-SIMS). Conversion of sputtering time to depth was done by measuring depth of the craters and assuming a linear sputter rate with degrading of the profiles edges due to sputter roughening within the craters.

The 7075 AA samples were measured using the quasi-continuous stiffness measurement (QCSM) module of ASMEC. This device stays in a vibration-free isolated cabinet and a Berkovich three-sided pyramidal diamond indenter was used for these measurements. Loading is stopped during a time interval of 3 s and the voltage for the piezoelectric element is overlaid with sinusoidal oscillations, which allows to obtain the depth dependent hardness values at the same position in the sample. Measurements with large differences to the others were excluded from the final analysis.

The nanofatigue tests were conducted in the same ASMEC equipment with a spherical diamond indenter (tip radius of 10 μm). Samples were subjected to cyclic contact tests by repeatedly indenting the same area at loads of 50-750 mN with minimum loads of 0.5-7.5 mN, respectively. These load values produce penetration depths of approximately 500-8,000 nm. Due to software limitations, no more than 300 cycles were allowed without the indenter leaving the surface. Thus, more indentations were performed in the same position to increase the number of cycles.

III. Results and Discussion

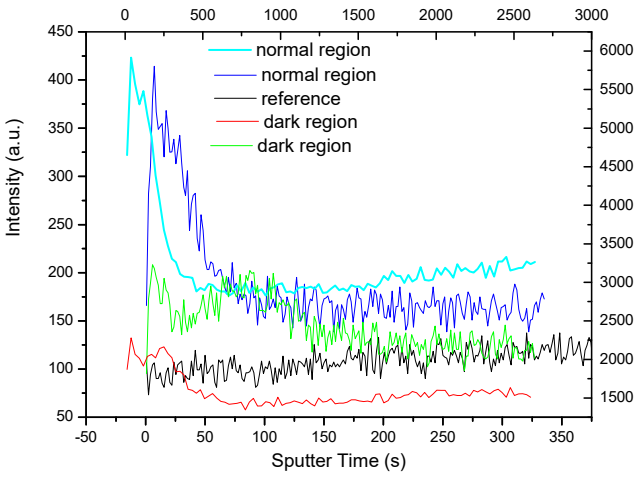

(a)

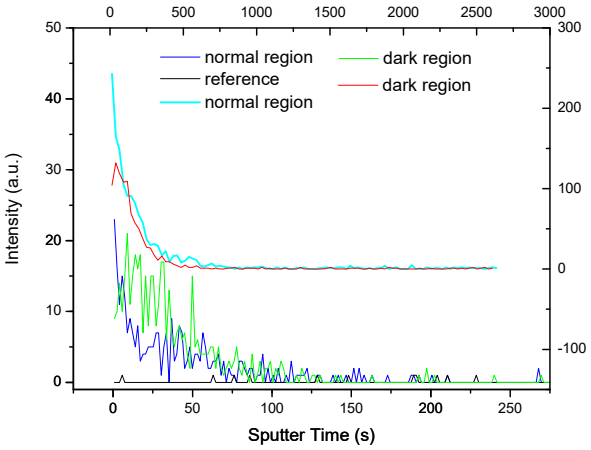

(b)

Fig. 1 SIMS results of 7075 AA samples: (a) oxygen and (b) nitrogen

The X-ray powder diffraction (XRD) measurements of the 7075 AA samples do not show any modifications after the PIII treatment. However, SIMS diagnostic detected nitrogen and oxygen at the surface (Fig. 1) with less than 10-nm depth. A dark region was visually observed in some samples because of

Open Science Index, Materials and Metallurgical Engineering Vol:11, No:3, 2017 publications.waset.org/10006624.pdf

the electric arc created by the shifted positioning of the protection shield at the front of the surface samples during the argon plasma cleaning process. This region suffered contamination, and thus, has different contents of many elements on the surface. The curves indicated as the normal region in Fig. 1 are relating to the PIII surface without the effect of the shifted positioning of the shield. Oxygen was less implanted because of such a problem in the shield; however, nitrogen was also not so affected.

As shown in Fig. 2, contaminants were pushed toward the surface by the ion implantation plus arc formation. This graphic is typical for all the other identified elements (around 30 including Li, B, Ti, etc.) that are present at very low intensity and a substantial depth.

Wear tests show a slight difference in the CoF (friction coefficient) between the treated and pristine surfaces, as visualized in Fig. 3 (a). The first six cycles with lower CoF's are due to the very thin aluminum oxide at the untreated surface. Even with a thicker layer for the treated surface, its removal time is identical to the untreated one and with a slightly higher CoF. After the layer removal, the coefficients are nearly the same, again with the treated one presenting higher values. This transition is inferred as the two-body abrasive mechanism passing to the three-body wear with the work-hardened debris acting as the micro-cutting chips. The wear mechanisms are abrasive and adhesive after 50 cycles, as identified by SEM, and the last one increasing after more than 50 cycles (total of 100). These wear tracks showed large plastic deformation and deeper ploughing line inside the track, as well as material pile-up at the edges.

Fig. 4 illustrates that the hardness profile of the aluminum alloy has shown again almost no modification because of the very thin layer obtained through PIII treatment. These results show no softening of the bulk, once a temperature of 200 ºC was not reached in the bulk. The low hardness at the surface can be attributed to contamination (forming an amorphous phase), roughness and high temperature at approximately up to 300 nm of depth. However, this technique presents high sensitivity, which in turn increases the variables allowing for an explanation of small variations [25]. For example, the more reasonable explanation for the hardness measurements, as shown in Fig. 4, is that it does not present the size, which could be effected by the high temperatures in this region of the material in the polishing operations.

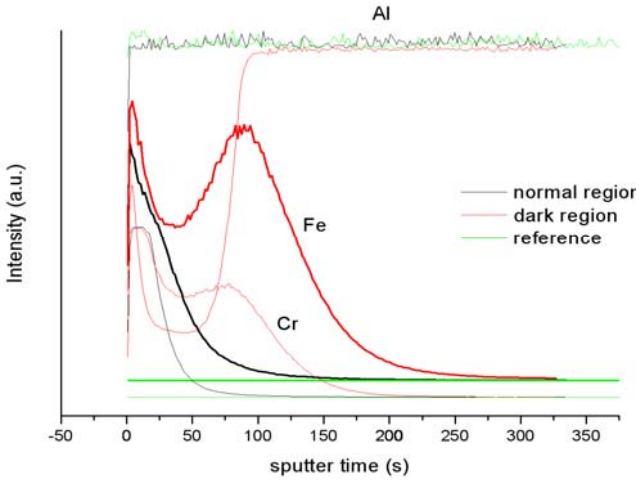

Fig. 2 SIMS results of 7075 AA samples

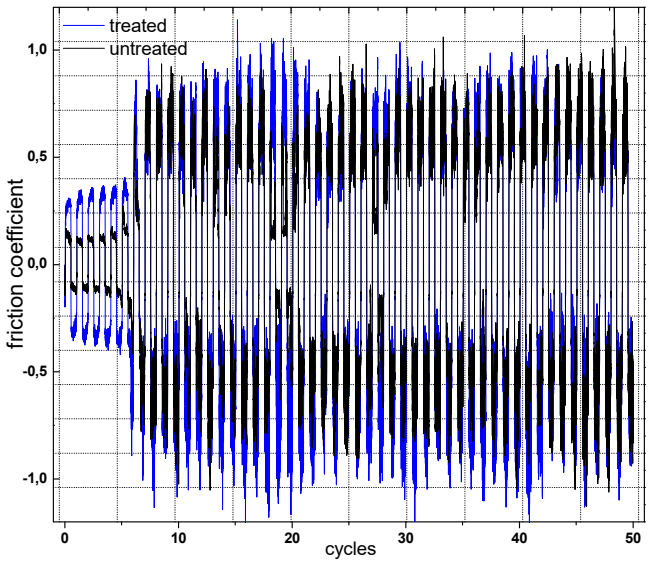

(a)

Open Science Index, Materials and Metallurgical Engineering Vol:11, No:3, 2017 publications.waset.org/10006624.pdf

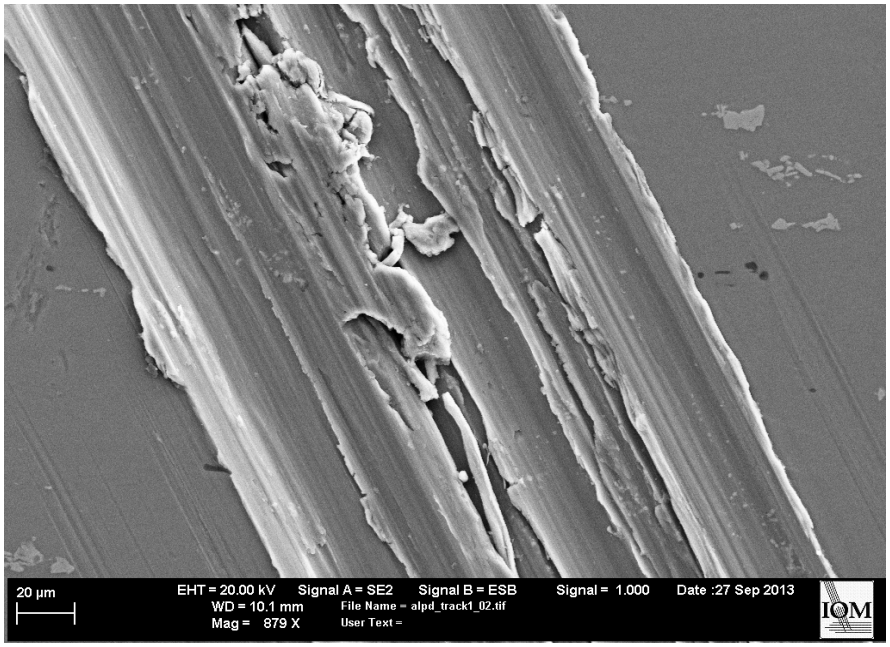

(b)

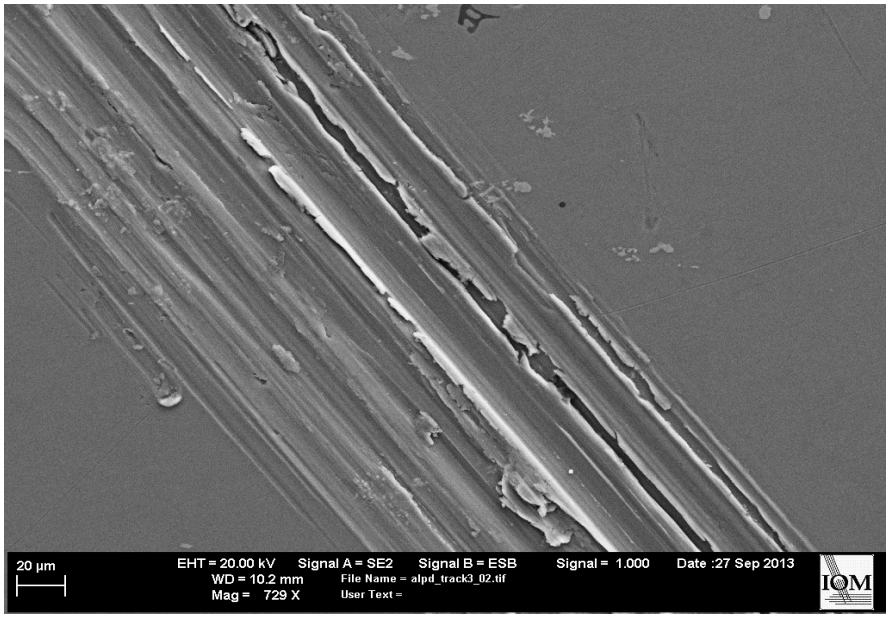

(c)

Fig. 3 (a) Friction coefficients, (b) tracks of untreated 7075 AA samples after 100 cycles, and (c) tracks of untreated 7075 AA samples after 50 cycles

Nanowear tests in this alloy produced large deformation with a load higher than 10 mN on both surfaces. At a load of 10 mN, the residual depth results totally from plastic deformation without material loss from crack fractures. Fig. 5 shows tracks resulted from 500 cycles of 100 mN with high plastic deformation generating cracks on the deformed material.

Like in another study [26], clear depth steps were not observed using the spherical indenter in nanofatigue experiments, which would be an indication of a sudden crack initiation. As stated by Alfredsson and Olsson [2], the initial stage of surface cracks formation produces depth changes too small to be captured reliably. Such a statement was related to microfatigue experiments, and also verified in the present work in nanoscale. However, some steps of more than 90 nm were identified in the experiments using 750 mN, which can be associated with crack formations.

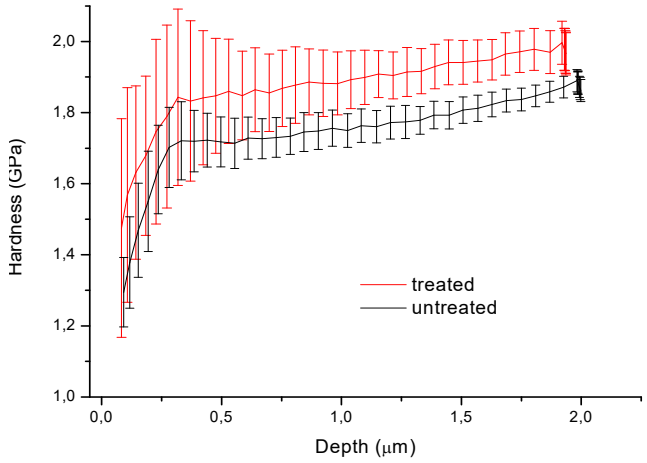

Fig. 4 QCSM results of 7075 AA

The differences between untreated and treated surfaces were indistinguishable because the adopted loads were chosen to produce indentations that could be visualized by SEM. During the first load cycle, the load-depth curve shows a hysteresis loop, which means the occurrence of plastic deformation. Such behavior is observed for loads above 50 mN, but this limit is lower and can be carefully further checked. Applying 50 mN, the registered maximum depth is around 650 nm, in which 150 nm are of elastic deformation (elastic/plastic ratio of 0.3). Using 750 mN, such depth is around 7,500 nm with 1000 nm of elastic deformation resulting in an elastic/plastic ration of 0.1. Ring cracks outside the indented area are observed at the surface after more than 20,000 cycles applying a maximum load of 750 mN (Fig. 6). Pile-up is observed with this relatively high load after only one cycle, indicating severe plastic deformation. No cracks are observed at the surface even after more than 50,000 cycles with 50-mN load.

Underneath a rounded indenter tip, the maximum shear stress in the material is a function of the load that nucleate a dislocation in a perfect crystal [6], which can be an explanation for the crosses observed in some indentations (Fig. 6). The film strength increases with decreasing film thickness because dislocations emitted from underneath, the indenter are slowed or otherwise hindered as they near some interfaces [6].

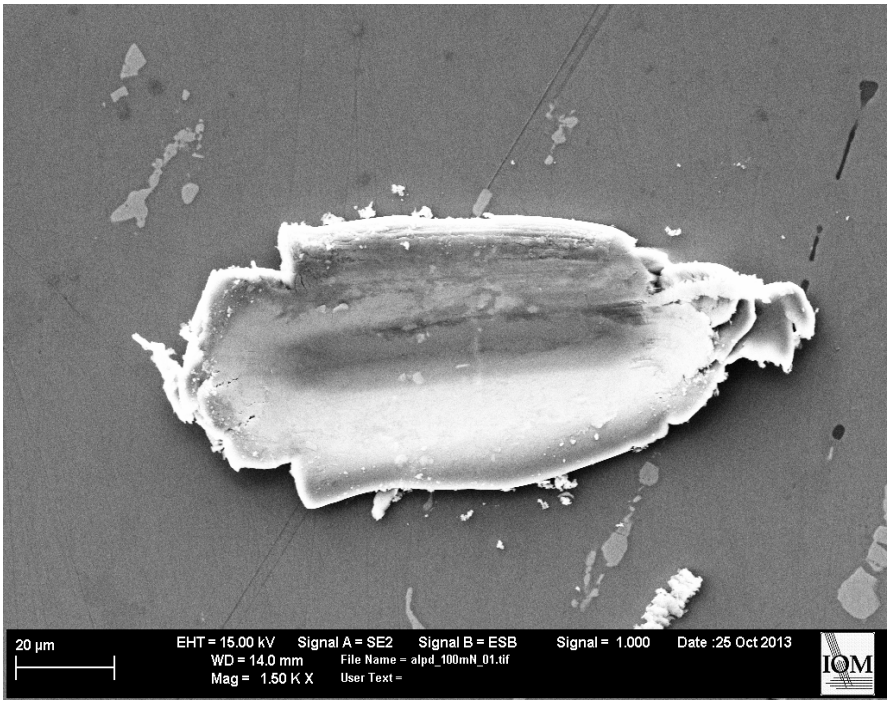

(a)

Open Science Index, Materials and Metallurgical Engineering Vol:11, No:3, 2017 publications.waset.org/10006624.pdf

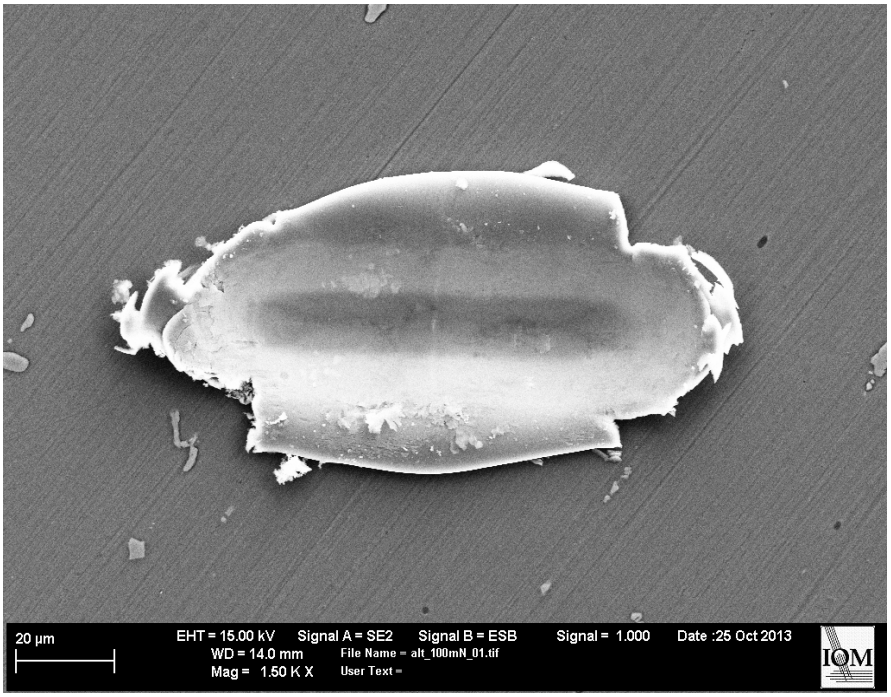

(b)

Fig. 5 Nanowear tracks created by 100-mN load on 7075 AA: (a) untreated, (b) treated

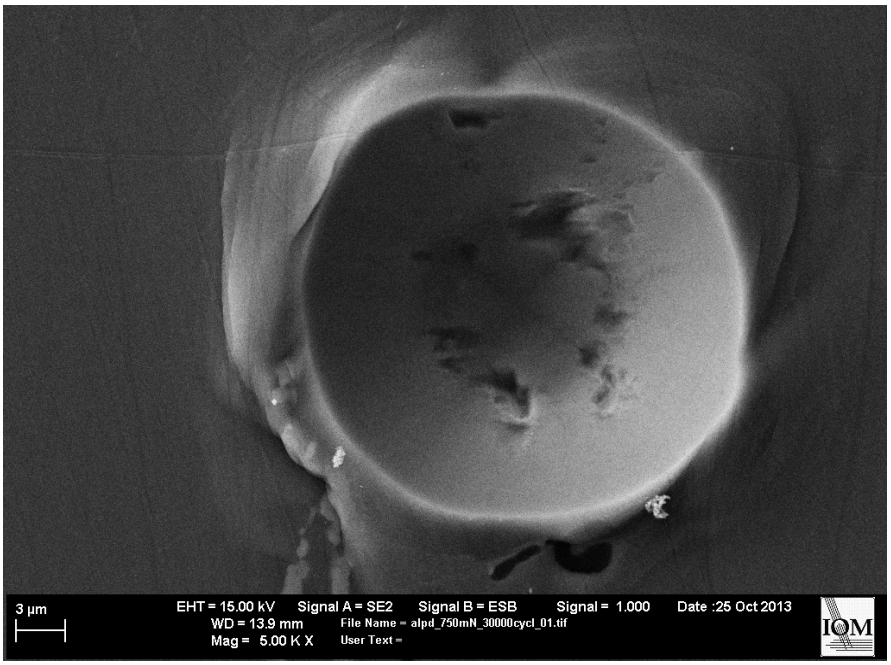

(a)

Open Science Index, Materials and Metallurgical Engineering Vol:11, No:3, 2017 publications.waset.org/10006624.pdf

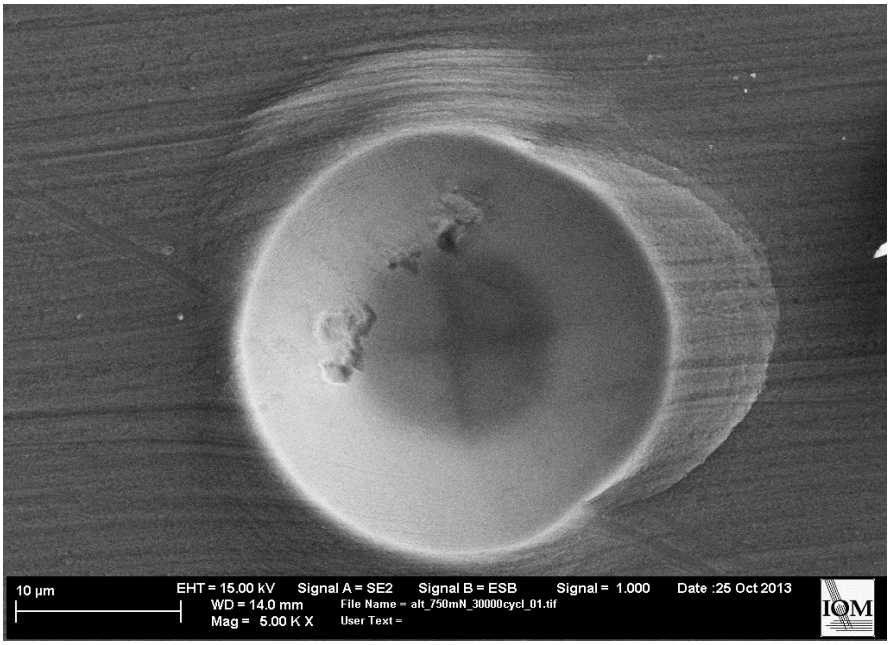

(b)

Fig. 6 Fatigue indentations on 7075 AA made from 30,000 cycles of 750-mN load: (a) untreated, (b) treated

IV. Conclusion

The very low nitrogen and oxygen concentrations that were implanted in the surface of 7075 AA samples have no significant effects on their nanomechanical and nanotribological properties. Such an implanted layer has an approximated thickness of 10 nm, as characterized by SIMS. Nanofatigue and nanowear experiments performed here aim to contribute to the development of such techniques, as they certainly will save samples that are necessary nowadays for such characterizations. Further tests must be performed to find more exact relations among the principal variables that are involved in the tension/deformation imposed by the spherical indenter.

The work herein presented physicochemical effects of electric arc on 7075 AA during PIII treatment, and also found that positioning of the shield must be improved to homogenize next treatments. Pulse duration larger than 4 µs must also be used in future experiments to increase the modified layer thickness. Anyway, the shallow layer produced here may be used as an anchor for other types of coatings [27].

Acknowledgments

We appreciate the financial support from the *CNPq*, *MCTI* and *FAPESP (*Sao Paulo Research Foundation*)* under grants # 2011/00872-2 and # 2012/21009-3.

References

[1] J. C. Williams, E. A. Starke Jr., Acta Mater. 51 (2003) 5775-5799.
[2] B. Alfredsson, M. Olsson. Fatigue Fract. Eng. Mater. Struct. 23 (2000) 229-240.
[3] E. Kral, K. Komvopoulos, D. B. Bogy. J. Appl. Mechanics. 60 (1993) 829-841.
[4] E. Valcheva, S. Dimitrov, D. Manova, S. Mändl, S. Alexandrova. Surf. Coat. Technol. 202 (2008) 2319-2322.
[5] S, Chen, L. Liu, T. Wang. Surf. Coat. Technol. 191 (2005) 25-32.
[6] K. J. Van Vliet, A. Gouldstone. Surf. Eng. 17 (2) (2001) 140-145.
[7] F. B. Abudaia, J. T. Evans, B. A. Shaw. Mater. Sci. Eng. A 391 (2005) 181-187.
[8] L. Marot, M. Drouet, F. Berneau, A. Straboni, Surf. Coat. Technol. 156 (2002) 155-158.
[9] C.B. Mello, M. Ueda, M.M. Silva, H. Reuther, L. Pichon, C.M. Lepienski. Wear 267 (2009) 867-873.
[10] R. M. Oliveira, C. B. Mello, G. Silva, J. A. N. Gonçalves, M. Ueda, L. Pichon. Surf. Coat. Technol. 205 (2011) S111-S114.
[11] H. –J. Spies, Surf. Eng. 26 (1-2) (2010) 126-134.
[12] D. Manova. Master Dissertation. Universität Augsburg, Augsburg, Germany, 2001.
[13] W. Ensinger, Surf. Coat. Technol. 100-101 (1998) 341-352.
[14] M. Ueda, H. Reuther, C. M. Lepienski, Nucl. Instr. Meth. Phys. Res. B 240 (2005) 199-203.
[15] K. G. Kostov, M. Ueda, M. Lepienski, P. C. Soares Jr., G. F. Gomes, M. M. Silva, H. Reuther, Surf. Coat. Technol. 186 (2004) 204-208.
[16] K. C. Walter, R. A. Dodd, J. R. Conrad, Nucl. Instr. Meth. Phys. Res. B 106 (1995) 522.
[17] S. Schoser, G. Bräuchle, J. Forget, K. Kohlhof, T. Weber, J. Voigt, B. Rauschenbach, Surf. Coat. Technol. 103-104 (1998) 222-226.
[18] G. Silva. M.Sc. Thesis. Technological Institute of Aeronautics, *São José dos Campos*, Brazil, 2007.
[19] G. S. Savonov. Ph.D. Thesis. Technological Institute of Aeronautics, *São José dos Campos*, Brazil, 2011.
[20] K. C. Walter, J. Vac. Sci. Technol. B 12 (2) (1994) 945-950.
[21] Z. Zhan, X. Ma, L. Feng, Y. Sun, L, Xia, Wear 220 (1998) 161-167.
[22] M. Ueda, A. R. Silva Jr., C. B. Mello, G. Silva, H. Reuther, V. S. Oliveira, Nucl. Instr. Meth. Phys. Res. B 269 (2011) 3246-3250.
[23] J. O. Rossi, M. Ueda, J. J. Barroso. IEEE Trans. Plasma Sci. 30 (5) (2002) 1622-1626.
[24] J. O. Rossi, J. J. Barroso, M. Ueda. IEEE Trans. Plasma Sci. 34 (5) (2006) 1846-1852.
[25] C.-L. Chen, A. Richter, R. Kögler, L.-T. Wu. J. Alloys Compds. 536S (2012) S194-S199.
[26] S. Saber-Samandari, K. A. Gross. Acta Biomater. 9 (2013) 5788-5794.
[27] M. Rahman. Ph.D. Thesis. Dublin City University, Dublin, Ireland, 2006.

Open Science Index, Materials and Metallurgical Engineering Vol:11, No:3, 2017 publications.waset.org/10006624.pdf